

# PET Imaging of Central 5-HT<sub>2A</sub> Receptors with Carbon-11-MDL 100,907

Hiroshi Ito, Svante Nyberg, Christer Halldin, Camilla Lundkvist and Lars Farde

Karolinska Institutet and Department of Clinical Neuroscience, Psychiatry Section, Karolinska Hospital, Stockholm, Sweden

Serotonergic 5-HT<sub>2A</sub> receptors are of central interest in the complex pathophysiology of schizophrenia. These receptors have also been proposed as putative targets for atypical antipsychotic drugs. Suitable radioligands for 5-HT<sub>2A</sub> receptors are required to evaluate this hypothesis in vivo with PET. MDL 100,907 is a highly selective 5-HT<sub>2A</sub> receptor antagonist that is currently being developed as a potential antipsychotic drug. We have previously reported on the preparation of [<sup>11</sup>C]MDL 100,907 and initial characterization of [<sup>11</sup>C]MDL 100,907 binding in the monkey brain. In this preliminary PET study, the regional distribution and binding kinetics of [<sup>11</sup>C]MDL 100,907 were examined in healthy men. **Methods:** A PET examination was performed in each of three subjects after intravenous injection of [<sup>11</sup>C]MDL 100,907. The metabolite-corrected arterial input function was used in a kinetic analysis according to the standard three-compartment model. **Results:** The highest radioactivity concentration was observed in the neocortex, whereas radioactivity was lower in the cerebellum, pons, thalamus, striatum and white matter. The binding potential (BP) in the neocortical regions was 4–6 times higher, whereas BP in the striatum was slightly higher than that in the cerebellum, demonstrating a regional distribution in good agreement with 5-HT<sub>2A</sub> receptor densities measured in vitro. The BP in the cerebellum was small but not negligible. **Conclusion:** This preliminary study suggests that [<sup>11</sup>C]MDL 100,907 is a suitable PET radioligand for studies on 5-HT<sub>2A</sub> receptors in man. The high selectivity of MDL 100,907 represents a major advantage as compared to presently available radioligands with poor selectivity. Thus, [<sup>11</sup>C]MDL 100,907 is recommended in the future for PET studies in healthy subjects and schizophrenic patients, including the determination of drug-induced 5-HT<sub>2A</sub> receptor occupancy.

**Key Words:** serotonergic receptor; brain; PET; schizophrenia

**J Nucl Med 1998; 39:208–214**

Serotonergic 5-HT<sub>2A</sub> receptors are of central interest in the complex pathophysiology of schizophrenia (1–4). The 5-HT<sub>2A</sub> receptor has also been proposed as a putative target for atypical antipsychotic drugs. This hypothesis is based on indirect pharmacological evidence and postmortem studies. To test the hypothesis further, suitable radioligands are required for direct studies in vivo of human brain 5-HT<sub>2A</sub> receptors with PET.

The spiperone derivative N-methylspiperone has been used as radioligand both for dopamine D2 and 5-HT<sub>2A</sub> receptors in man (5,6). More recently, radioligands such as [<sup>18</sup>F]altanserin and [<sup>18</sup>F]setoperone have been explored (7,8). However, none of the currently available radioligands have proved to be ideal. They all bind with a rather low specific-to-nonspecific binding ratio. Moreover, they are not selective for the 5-HT<sub>2A</sub> receptor, all having considerable affinity for other neuroreceptors, such as the D2 dopamine and  $\alpha_1$ -adrenergic subtypes (9,10).

MDL 100,907 (Fig. 1) is a potent and highly selective 5-HT<sub>2A</sub> receptor antagonist that is currently being developed as a potential atypical antipsychotic drug (11–13). In vitro, MDL 100,907 binds with subnanomolar affinity to 5-HT<sub>2A</sub> receptors

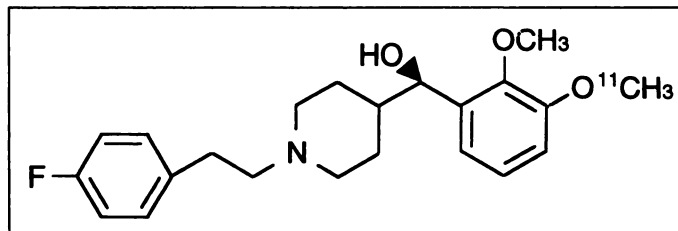


**FIGURE 1.** The chemical structure of [<sup>11</sup>C]MDL 100,907 [(R)-(+)-4-(1-hydroxy-1-(2,3-dimethoxyphenyl)ethyl)-N-2-(4-fluorophenylethyl) piperidine].

(K<sub>i</sub> = 0.2 nM), whereas its affinity for other putative receptors is at least 100-fold lower. In addition, its moderate lipophilicity [logP of 2.7] and molecular structure enabling <sup>11</sup>C-methylation of the corresponding 3-hydroxyl precursor (MDL 105,725) identifies MDL 100,907 as a potential PET radioligand for examination of 5-HT<sub>2A</sub> receptors.

We recently reported on the preparation of [<sup>11</sup>C]MDL 100,907 and initial PET measurements in monkeys (14). In monkey brain, [<sup>11</sup>C]MDL 100,907 bound specifically and reversibly to 5-HT<sub>2A</sub> receptors. The specific-to-nonspecific binding ratio was high (3.5–4.5). Here, the regional distribution and binding kinetics of [<sup>11</sup>C]MDL 100,907 were studied to evaluate its suitability as a PET radioligand for 5-HT<sub>2A</sub> receptors in man.

## MATERIALS AND METHODS

### Subjects

The study was approved by the Ethics and the Radiation Safety Committees of the Karolinska Hospital and the Medical Products Agency of Sweden. Three healthy men (ages 20, 23 and 35 yr) were recruited and gave written informed consent. The subjects were healthy according to medical history, physical examination, blood and urine screening analyses, and magnetic resonance imaging (MRI) of the brain. They did not use any medication.

### Radiochemistry

Carbon-11-MDL 100,907 was synthesized as recently reported (14). The demethylated precursor, MDL 105,725, was provided by A.A. Carr (Hoechst Marion Roussel, Cincinnati, OH). Carbon-11-MDL 100,907 was obtained by methylation of MDL 105,725 using [<sup>11</sup>C]methyl iodide (Fig. 1). The specific radioactivity of [<sup>11</sup>C]MDL 100,907 at time of administration was 10–20 GBq/ $\mu$ mol.

### PET Experimental Procedure

After intravenous bolus injection of 302–358 MBq [<sup>11</sup>C]MDL 100,907, brain radioactivity was measured in a consecutive series of time frames for up to 93 min. The frame sequence consisted of nine 20-sec frames, six to ten 3-min frames, four to six 6-min frames and up to three 12-min frames. The PET system used was Siemens ECAT Exact HR, which provides 47 sections with a center-to-center distance of 3.125 mm (15). The in-plane and axial resolutions are 3.8 mm and 4.0 mm, respectively, FWHM. A head fixation system with an individual plaster helmet was used both in

Received Nov. 25, 1997; revision accepted Apr. 7, 1997.

For correspondence or reprints contact: Hiroshi Ito, MD, Department of Clinical Neuroscience, Psychiatry Section, Karolinska Hospital, S-171 76 Stockholm, Sweden.

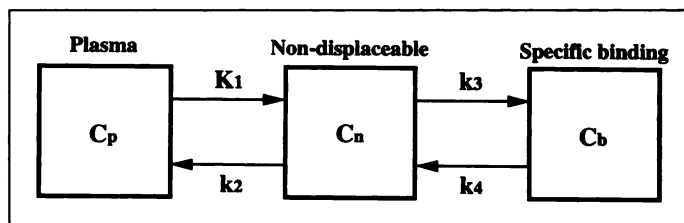


**FIGURE 2.** The three-compartment model used to describe the kinetics of [<sup>11</sup>C]MDL 100,907 binding in brain.

the PET and MRI experiments to allow a master of positioning between the two modalities (16).

To obtain the arterial input function, an automated blood sampling system was used during the first 5 min of each PET experiment (17). Thereafter, arterial blood samples were taken manually at the midpoint of each frame until the end of the measurement (18). The fraction of radioactivity representing unchanged [<sup>11</sup>C]MDL 100,907 in plasma was determined by gradient high-performance liquid chromatography (HPLC), as described previously (14,19,20).

### Regions of Interest

T2-weighted and proton density MR images of the brain were obtained for all subjects. The MRI system used was GE Signa (Milwaukee, WI) (1.5 T). The positioning of the head and the series of sections were the same as those in the PET studies. Regions of interest (ROIs) were drawn on the MR images and transferred to the reconstructed PET images. ROIs were defined for cerebellar cortex, pons, thalamus, caudate, putamen and five neocortical regions, representing the frontal, temporal, parietal and occipital lobes and the cingulate gyrus. Each ROI was drawn in four adjacent sections, and data were pooled to obtain the average radioactivity concentration for the whole volume of interest. To obtain regional time-activity curves, regional radioactivity was calculated for each frame, corrected for decay and plotted against time.

### Kinetic Analysis

The time-activity curves of several neuroreceptor ligands have been described using the standard three-compartment model with four first-order rate constants (18,21–23). Three compartments are defined as follows (Fig. 2):

1. The radioactivity concentration of unchanged radioligand in plasma ( $C_p$ );
2. The radioactivity concentration of nondisplaceable radioligand in brain ( $C_n$ ); and
3. The radioactivity concentration of radioligand specifically bound to receptors ( $C_b$ ).

All concentrations are in the units nCi/ml. It is assumed that all compartments are homogeneous in concentration. The rate constants  $K_1$  and  $k_2$  correspond to the influx and efflux rates for radioligand diffusion through the blood-brain barrier, respectively. The rate constants  $k_3$  and  $k_4$  correspond to the rates for radioligand transfer between the compartments for nondisplaceable and specific radioligand binding to receptors, respectively. On the basis of this model, the following differential equations can be expressed:

$$dC_n(t)/dt = K_1 \cdot C_p(t) - (k_2 + k_3) \cdot C_n(t) + k_4 \cdot C_b(t), \quad \text{Eq. 1}$$

$$dC_b(t)/dt = k_3 \cdot C_n(t) - k_4 \cdot C_b(t) \quad \text{Eq. 2}$$

and

$$C_t(t) = C_n(t) + C_b(t), \quad \text{Eq. 3}$$

where  $C_t(t)$  is the radioactivity concentration in brain as measured by PET.

A widely used quantitative approach has been to express radioligand binding in terms of distribution volume concepts (24). Two such volumes are defined by Equations 4 and 5:

$$V_n = K_1/k_2 \quad \text{Eq. 4}$$

and

$$V_t = (K_1/k_2) \cdot (1 + k_3/k_4). \quad \text{Eq. 5}$$

$V_n$  is the distribution volume in a brain region with only nondisplaceable binding and, thus, is devoid of specific binding sites.  $V_t$  is the total distribution volume and has been used as a quantitative measure for the binding of radioligands with low interindividual variability in  $V_n$ . To calculate  $V_n$  and  $V_t$ , the rate constants obtained from the three-compartment model were entered into Equations 4 and 5.

The three-compartment model analysis is based on the use of a radioligand with high specific radioactivity. At such conditions, the receptor density ( $B_{max}$ ) and affinity ( $K_d$ ) cannot be differentiated (18,21,22). The ratio  $B_{max}/K_d$  corresponds to the ratio  $k_3/k_4$  and is often referred to as the binding potential (BP):

$$B_{max}/K_d = (k_3/k_4) \cdot (1/f_2), \quad \text{Eq. 6}$$

where  $f_2$  is the free fraction of radioligand in the nondisplaceable compartment.

### Nonlinear Least Squares Fitting Analysis

The three-compartment model was used in an initial attempt to describe the time-activity curves for regional [<sup>11</sup>C]MDL 100,907 binding. The traditional strategy is to estimate rate constants by nonlinear least squares fitting (NLLSF) to the regional time-activity curves (25). The model equations (Eqs. 1 and 2) were combined and solved in a convolution integral procedure and then used for the NLLSF analysis. The radioactivity of unchanged [<sup>11</sup>C]MDL 100,907 in plasma was used as the arterial input function (18).

In a numerical analysis, variation is reduced by the use of fewer parameters. Thus, two manners of the NLLSF analysis were performed for each regional time-activity curve. The first analysis included the estimation of four rate constants ( $K_1$ ,  $k_2$ ,  $k_3$  and  $k_4$ ). The second analysis included that three rate constants were estimated [ $K_1$ ,  $k_3$  and  $k_4$  ( $k_2 = K_1/V_n$ )] assuming the  $V_n$  value calculated from  $K_1$  and  $k_2$  values of the cerebellum (26).

The cerebellum is a region with low density of 5-HT<sub>2A</sub> receptors (27–29). In a region with no specific binding sites, the two-compartment model with two rate constants, which does not have specific binding compartment ( $C_b$ ), should be sufficient to describe the time-activity curves. To evaluate if specific binding in the cerebellum can be regarded as negligible, both a two-compartment and a three-compartment model were applied for this region (18). To compare the two models, three statistical methods were used: the Akaike information criterion (30), the Schwarz criterion (sulfur chloride) (31) and F statistics (32).

Two approaches were applied to correct for the effect of cerebral blood volume (CBV). The first was to exclude the first four frames (0–80 sec) of the regional time-activity curves (33). The second was to use reference values for regional CBV (34) and the curve for measured radioactivity in arterial whole blood. The radioactivity in CBV calculated in this way was then subtracted from the regional time-activity curves before the kinetic analyses. The rate constants obtained by both approaches were compared for cross-validation purposes.

### Graphical Analysis

The total distribution volume ( $V_t$ ) was also calculated using the graphical analysis developed by Logan et al. (35). This analysis has been developed for reversible ligands and allows for the calculation

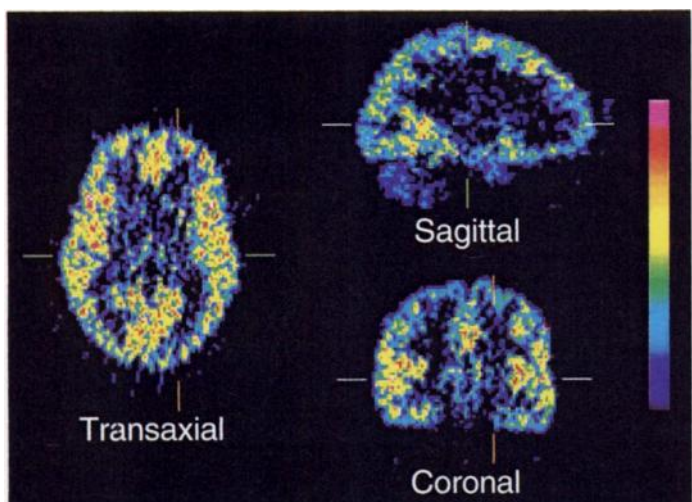


**FIGURE 3.** PET images of Subject B in three dimensions, obtained by summation of the frames from 39–81 min after intravenous injection of [ $^{11}\text{C}$ ]MDL 100,907. The subject's right hemisphere is to the left of the figure in the transaxial and coronal sections. The anterior is to the right of the figure in the sagittal section.

of  $V_t$  by using simple linear least squares fitting, which requires less calculation time. The radioactivity of unchanged [ $^{11}\text{C}$ ]MDL 100,907 in plasma was used as the arterial input function (18).

## RESULTS

After intravenous injection of [ $^{11}\text{C}$ ]MDL 100,907, the radioactivity appeared rapidly in brain. The highest radioactivity concentrations were observed in the neocortex, whereas radioactivity was lower in the cerebellum, pons, thalamus, striatum and white matter (Fig. 3).

The time courses for regional brain radioactivity are shown in Figure 4. The radioactivity concentrations were on a similar level among all neocortical regions and reached a plateau after about 40 min. In all subjects, the ratios of radioactivity in the neocortical regions to the cerebellum were 1.6–2.1 at 54 min after injection.

The blood and plasma curves are shown in Figure 5. The whole blood-to-plasma radioactivity ratio remained constant

with time and ranged from 1.64–1.66 in the three subjects. In the repeated HPLC analyses, the parent compound and polar metabolites could readily be identified in all subjects. However, in Subject A, the HPLC analysis did not permit accurate quantification of the parent compound. Therefore, a slightly modified HPLC method was used in Subjects B and C. The fraction of unchanged [ $^{11}\text{C}$ ]MDL 100,907 in plasma was about 95% at 4 min and about 40% at 50 min after injection in Subjects B and C. The average values of unchanged [ $^{11}\text{C}$ ]MDL 100,907 in plasma for Subjects B and C were used to calculate the arterial input function for Subject A.

The time-activity curves for all regions, including the cerebellum, were well described by the three-compartment model (Fig. 6). The uptake curve for the cerebellum was not adequately described by the two-compartment model (Fig. 6 and Table 1). In the statistical analyses, the Akaike information criterion and Schwarz criterion scores were lower for the three-compartment model than they were for the two-compartment model, indicating the three-compartment model to be the preferred model for the cerebellum. Moreover, F statistics rejected the null hypothesis, i.e., that the two-compartment model more adequately describes radioligand uptake for the cerebellum, at the 1% level for Subjects A and B and at the 0.1% level for Subject C.

The rate constants obtained by NLLSF analyses using the three-compartment model are shown in Tables 2 and 3. Reversibility of binding was indicated by  $k_4$  values well above zero. The BP ( $k_3/k_4$ ) for the neocortical regions were 4–6 times higher, whereas the BP in the putamen and caudate were slightly higher than those in the cerebellum. In the NLLSF analyses, similar results were obtained using three and four rate constants (Table 2). Both approaches applied to correct for the effect of CBV gave almost identical results in the kinetic analysis (data not shown).

In the graphical analysis, a linear phase was observed from 42 min to end of measurement for all regions including the cerebellum (Fig. 7). The slope of the fitted line corresponds to  $V_t$ . The observation that the slope was not infinite indicates that [ $^{11}\text{C}$ ]MDL 100,907 binding is reversible. The  $V_t$  values ob-

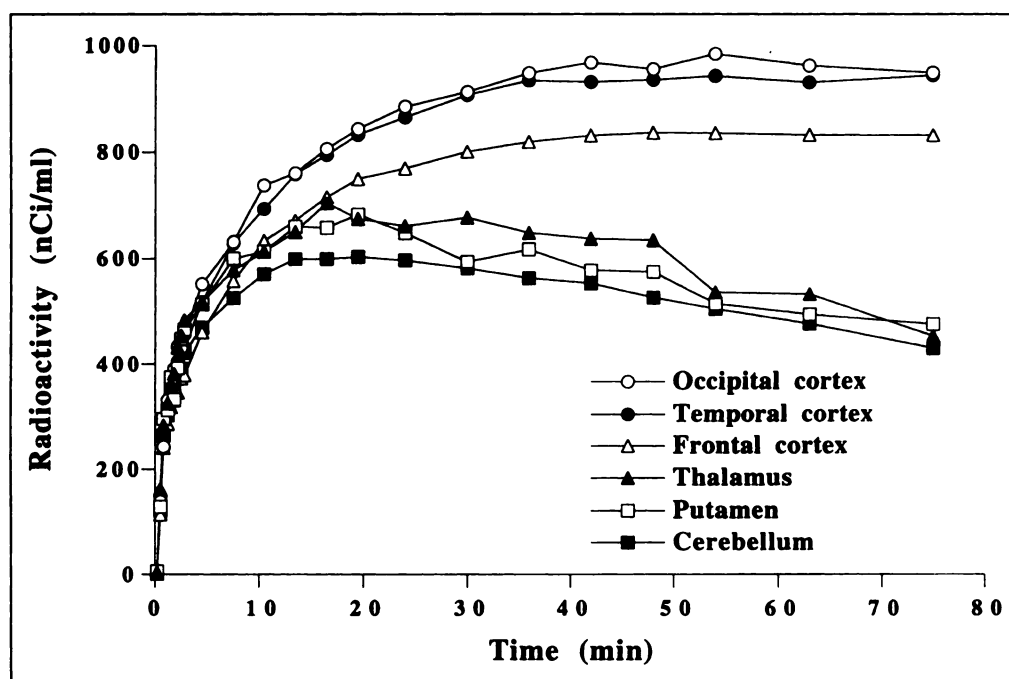


**FIGURE 4.** Time-activity curves for regional brain radioactivity after intravenous injection of 357 MBq [ $^{11}\text{C}$ ]MDL 100,907 in Subject B.

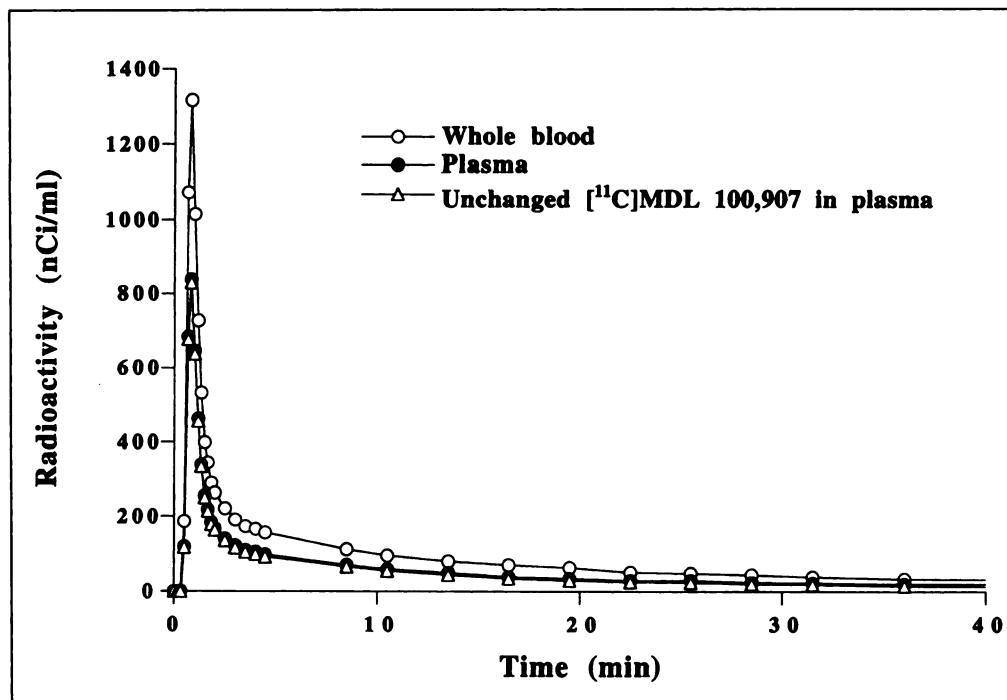


**FIGURE 5.** Time-activity curves for radioactivity in whole blood and plasma and the time-activity curve for unchanged [<sup>11</sup>C]MDL 100,907 in plasma of Subject B.

tained by NLLSF analyses were consistent with those obtained by the graphical analysis (data not shown).

## DISCUSSION

### Binding Characteristics of Carbon-11-MDL 100,907

Carbon-11-MDL 100,907 has a high affinity and selectivity for the 5-HT<sub>2A</sub> receptor *in vitro* (11–13). The specificity of [<sup>11</sup>C]MDL 100,907 for 5-HT<sub>2A</sub> receptors has recently been confirmed by PET *in vivo* in the monkey brain (14).

After intravenous injection of tracer doses of [<sup>11</sup>C]MDL 100,907, radioactivity was high in all neocortical regions and low in the cerebellum, pons, thalamus, striatum and white matter (Fig. 3). The BP in the neocortical regions was considerably higher, whereas the BP in the putamen and caudate was

slightly higher than it was in the cerebellum (Tables 2 and 3). This regional distribution is actually in good agreement with the known distribution of 5-HT<sub>2A</sub> receptors (27–29) and clearly supports that the ligand binds selectively to 5-HT<sub>2A</sub> receptors in the human brain.

Reversibility of binding was supported by the graphical analysis, the slope of the fitted line not approaching infinity (Fig. 7). Reversibility was further supported by *k*<sub>4</sub> values well above zero in the NLLSF analysis (Table 2). These observations are consistent with results of displacement experiments in monkey brain (14).

The radioactivity in whole blood was higher than it was in plasma (Fig. 5). This is an uncommon observation because other radioligands commonly show higher radioactivity in

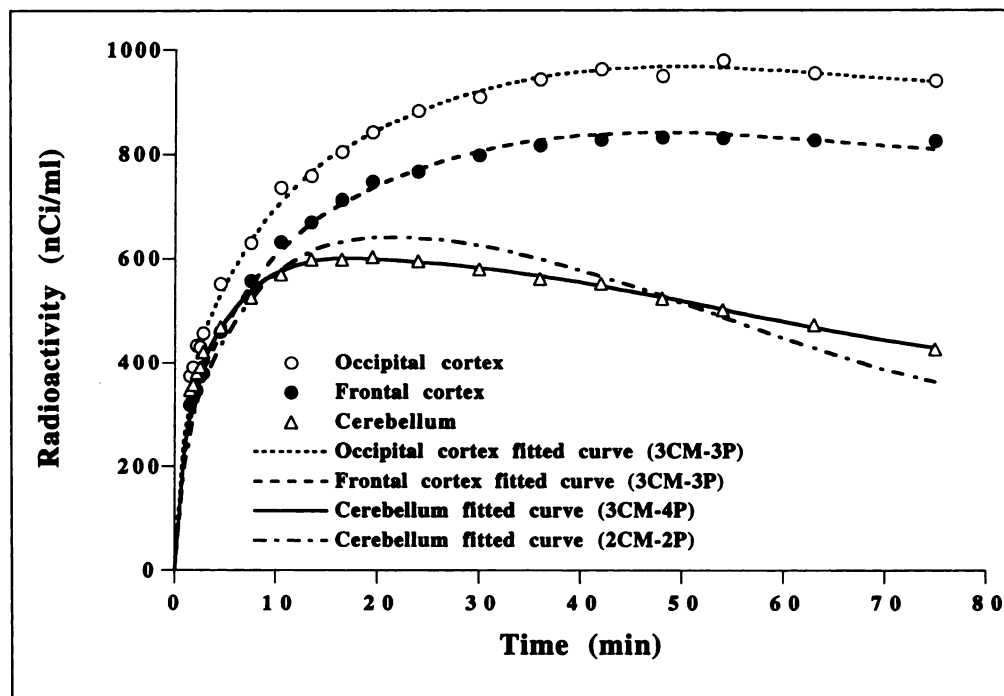


**FIGURE 6.** Experimental values for regional radioactivity and the corresponding fitted curves obtained by analyses by the two-compartment model with two rate constants (2CM-2P) or the three-compartment model with three (3CM-3P) or four (3CM-4P) rate constants in Subject B.

**TABLE 1**  
Results for the Cerebellum in Three Healthy Subjects Obtained by Nonlinear Least Squares Fitting Analyses\*

	$K_1$ (ml/ml/min)	$k_2$ ( $\text{min}^{-1}$ )	$k_3$ ( $\text{min}^{-1}$ )	$k_4$ ( $\text{min}^{-1}$ )	AIC	SC	p value
Subject A							
2CM-2P	0.503	0.026	—	—	125	127	
3CM-4P	0.572	0.060	0.050	0.025	113	117	
F statistics							<0.01
Subject B							
2CM-2P	0.485	0.021	—	—	142	144	
3CM-4P	0.569	0.055	0.044	0.021	127	131	
F statistics							<0.01
Subject C							
2CM-2P	0.480	0.019	—	—	125	127	
3CM-4P	0.557	0.066	0.082	0.030	89	93	
F statistics							<0.001

\*Three statistical methods were used to select the most adequate model. The AIC and SC give a number for each model. The lowest number indicate the preferred model. For the F statistics the null hypothesis was that the two-compartment model more adequately describes radioligand uptake. The p value indicates what level upon which the null hypothesis was rejected.

2CM-2P = two-compartment model with two rate-constants; 3CM-4P = three-compartment model with four rate-constants; AIC = Akaike information criterion; SC = Schwarz criterion.

plasma than they do in the whole blood. It is speculated that [ $^{11}\text{C}$ ]MDL 100,907 may bind to the 5-HT<sub>2A</sub> receptors, which are abundant in platelet membranes (36).

### Cerebellum

The quantification of neuroreceptors using a reference region is a conventional approach for applied clinical neuroimaging. The cerebellum has previously been used as a reference region for determination of 5-HT<sub>2A</sub> receptors in PET studies using [ $^{11}\text{C}$ ]N-methylspiperone (5,6), [ $^{18}\text{F}$ ]altanserin (8) and [ $^{18}\text{F}$ ]se-

toperone (37), despite the known presence of 5-HT<sub>2A</sub> receptors, as demonstrated in vitro (27–29). However, the assumption of negligible radioligand binding in the cerebellum has not been well validated in previous PET studies. In this study, the two-compartment model could not describe the data for the cerebellum, whereas the three-compartment model was adequate (Fig. 6 and Table 1). The BP value of the cerebellum was small but not negligible (Tables 2 and 3). These observations may support the view that there is specific binding to 5-HT<sub>2A</sub>

**TABLE 2**  
Rate Constant Range Obtained by Both Nonlinear Least Squares Fitting Analyses in Three Healthy Subjects\*

Region	$K_1$ (ml/ml/min)	$k_2$ ( $\text{min}^{-1}$ )	$k_3$ ( $\text{min}^{-1}$ )	$k_4$ ( $\text{min}^{-1}$ )	$k_3/k_4$
Frontal cortex					
3CM-4P	0.52–0.55	0.03–0.04	0.08–0.22	0.01–0.02	5.8–8.8
3CM-3P	0.53–0.56	0.05–0.07	0.16–0.33	0.02–0.02	7.5–13.9
Temporal cortex					
3CM-4P	0.51–0.60	0.04–0.07	0.12–0.30	0.01–0.03	8.9–13.3
3CM-3P	0.52–0.61	0.05–0.07	0.17–0.26	0.02–0.02	9.4–13.2
Parietal cortex					
3CM-4P	0.50–0.55	0.05–0.06	0.18–0.28	0.02–0.03	7.3–13.4
3CM-3P	0.51–0.55	0.05–0.07	0.18–0.29	0.02–0.03	7.2–14.5
Occipital cortex					
3CM-4P	0.67–0.70	0.08–0.11	0.16–0.33	0.01–0.02	9.9–15.9
3CM-3P	0.64–0.66	0.06–0.08	0.16–0.26	0.02–0.02	8.0–12.0
Cingulate gyrus					
3CM-4P	0.60–0.65	0.05–0.09	0.10–0.25	0.01–0.02	8.2–15.5
3CM-3P	0.60–0.65	0.06–0.08	0.11–0.24	0.01–0.03	8.9–13.8
Putamen					
3CM-4P	0.60–0.64	0.06–0.08	0.06–0.09	0.02–0.04	1.6–3.4
3CM-3P	0.58–0.63	0.06–0.08	0.05–0.07	0.02–0.03	2.1–3.1
Caudate					
3CM-4P	0.54–0.62	0.04–0.07	0.02–0.12	0.01–0.05	2.3–3.0
3CM-3P	0.56–0.61	0.06–0.07	0.06–0.12	0.02–0.05	2.5–2.6
Thalamus					
3CM-4P	0.53–0.64	0.04–0.07	0.05–0.11	0.04–0.04	1.3–2.6
3CM-3P	0.54–0.63	0.06–0.07	0.07–0.12	0.04–0.06	1.8–2.9
Pons					
3CM-4P	0.41–0.46	0.04–0.11	0.03–0.12	0.01–0.03	1.8–4.2
3CM-3P	0.40–0.44	0.04–0.05	0.03–0.04	0.01–0.02	1.8–2.7
Cerebellum					
3CM-4P	0.56–0.57	0.05–0.07	0.04–0.08	0.02–0.03	2.0–2.7

\*3CM-4P = three-compartment model with four rate constants; 3CM-3P = three-compartment model with three rate constants.

**TABLE 3**

Values Obtained by Nonlinear Least Squares Fitting Analysis Using Three-Compartment Model with Three or Four Rate Constants in Three Healthy Subjects

Region	$V_n$ (ml/ml)*	$k_3/k_4$	$V_t$ (ml/ml)†
Subject A			
Frontal cortex	9.6	7.5	81
Temporal cortex	9.6	10.8	113
Occipital cortex	9.6	8.0	86
Cerebellum	9.6	2.0	29
Subject B			
Frontal cortex	10.4	7.9	92
Temporal cortex	10.4	9.4	108
Occipital cortex	10.4	10.2	116
Cerebellum	10.4	2.1	32
Subject C			
Frontal cortex	8.4	13.9	125
Temporal cortex	8.4	13.2	119
Occipital cortex	8.4	12.0	109
Cerebellum	8.4	2.7	31

\* $V_n = K_1/k_2$ .

† $V_t = (K_1/k_2) \cdot (1 + k_3/k_4)$ .

receptors in this region. On the other hand, the failure of the two-compartment model to describe the time-activity curves in the cerebellum could also be explained if [<sup>11</sup>C]MDL 100,907 has a lipophilic metabolite that might transfer across the blood-brain barrier and contribute to the radioactivity concentration of the cerebellum. In Subjects B and C, a small peak that might correspond to such a metabolite was observed during the late phase of the PET measurement. This preliminary observation is not supported by metabolism studies in vitro (Hoechst Marion Roussel, data on file). Thus, to explain the three-compartment model, the presence of a low density of 5-HT<sub>2A</sub> receptors in the cerebellum appears to be the most likely hypothesis.

**Clinical Application**

The time-activity curves for all regions were well described by the three-compartment model. A high BP was observed in

the neocortical regions. These observations suggest that [<sup>11</sup>C]MDL 100,907 should be suitable for quantitative determination of 5-HT<sub>2A</sub> receptors. In the absence of an ideal reference region, an arterial input function is required for accurate quantification of 5-HT<sub>2A</sub> receptors using [<sup>11</sup>C]MDL 100,907. The high selectivity of MDL 100,907 represents a major advantage, as compared to presently available radioligands with poor selectivity. Thus, [<sup>11</sup>C]MDL 100,907 is recommended in the future for PET studies in healthy subjects and schizophrenia patients, including the determination of drug-induced 5-HT<sub>2A</sub> receptor occupancy.

Several new antipsychotic compounds with high affinity for 5-HT<sub>2A</sub> receptors are presently coming into clinical use. The development of such compounds is based on the hypothesis that the 5-HT<sub>2A</sub> receptor antagonism may be beneficial in the treatment of schizophrenia, especially for negative symptoms. This hypothesis can be tested by a search for correlations between central 5-HT<sub>2A</sub> receptor binding and clinical efficacy in treated patients. Of particular interest is that MDL 100,907 is now being evaluated as a potential antipsychotic in an extensive clinical research program. In this study, we have shown that [<sup>11</sup>C]MDL 100,907 is a suitable PET radioligand for studies on 5-HT<sub>2A</sub> receptors in man. Thus, [<sup>11</sup>C]MDL 100,907 offers a unique opportunity to correlate the clinical pharmacology of selective 5-HT<sub>2A</sub> receptor antagonism to detailed in vivo characterization of 5-HT<sub>2A</sub> receptor binding.

**CONCLUSION**

Here, the regional distribution and binding kinetics of [<sup>11</sup>C]MDL 100,907 were examined in healthy men. The time-activity curves for all regions were well described by the three-compartment model. The regional distribution was in good agreement with 5-HT<sub>2A</sub> receptor densities demonstrated in vitro. Its high selectivity represents a major advantage as compared to presently available radioligands. Thus, [<sup>11</sup>C]MDL 100,907 is recommended for PET studies in the future.

**ACKNOWLEDGMENTS**

This work was supported by Swedish Medical Research Council Grant 09114-0613, Swedish Natural Science Research Council

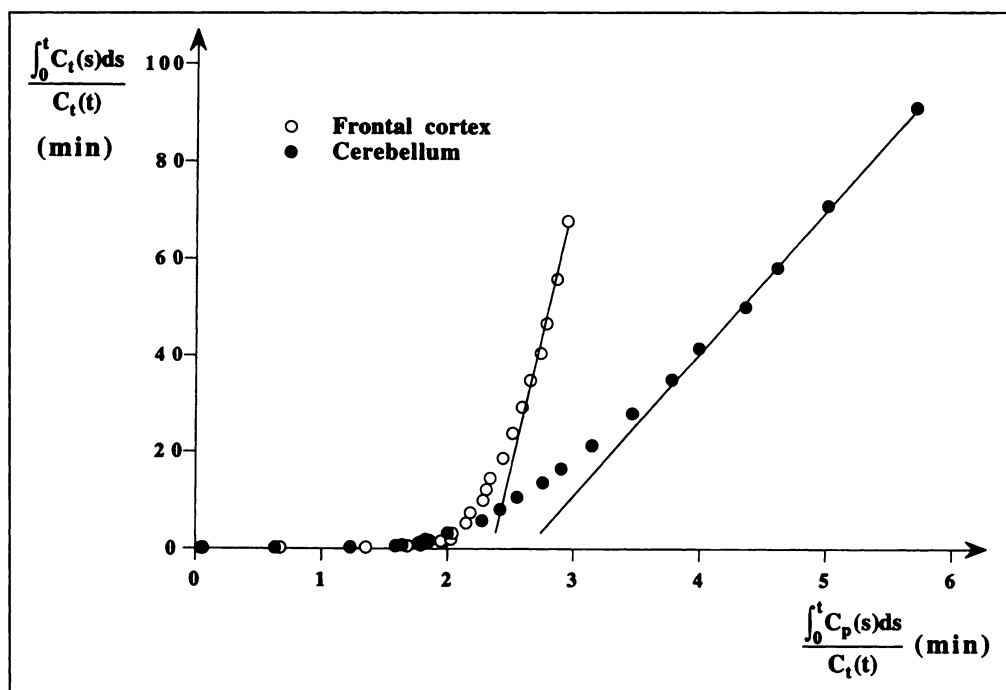


**FIGURE 7.** Linear graphical analyses of [<sup>11</sup>C]MDL 100,907 binding in the frontal cortex and the cerebellum of Subject B.

Grant K-KU 9973-307, National Institute of Mental Health Grant 41205-10, the Karolinska Institutet and Hoechst Marion Roussel. The assistance of the members of the Karolinska PET group involved in the PET experiments is also gratefully acknowledged.

## REFERENCES

- Meltzer HY. Clinical studies on the mechanism of action of clozapine: the dopamine-serotonin hypothesis of schizophrenia. *Psychopharmacology* 1989;99(suppl):S18-S27.
- Csemansky JG, Poscher M, Faull KF. Serotonin in schizophrenia. In: Coccaro EF, Murphy DL, eds. *Serotonin in major psychiatric disorders*. Washington, DC: American Psychiatric Press; 1990:209-230.
- Schmidt CJ, Sorensen SM, Kehne JH, Carr AA, Palfreyman MG. The role of 5HT<sub>2A</sub> receptors in antipsychotic activity. *Life Sci* 1995;56:2209-2222.
- Svensson TH, Mathé JM, Andersson JL, Nomikos GG, Hildebrand BE, Marcus M. Mode of action of atypical neuroleptics in relation to the phencyclidine model of schizophrenia: role of 5-HT<sub>2</sub> receptor and alpha 1-adrenoreceptor antagonism. *J Clin Psychopharmacol* 1995;15:11S-18S.
- Wong DF, Wagner HN Jr, Dannals RF, et al. Effects of age on dopamine and serotonin receptors measured by positron tomography in the living human brain. *Science* 1984;226:1393-1396.
- Nyberg S, Farde L, Eriksson L, Halldin C, Eriksson B. 5-HT<sub>2</sub> and D<sub>2</sub> dopamine receptor occupancy in the living human brain. A PET study with risperidone. *Psychopharmacology* 1993;110:265-272.
- Blin J, Sette G, Fiorelli M, et al. A method for the in vivo investigation of the serotonergic 5-HT<sub>2</sub> receptors in the human cerebral cortex using positron emission tomography and <sup>18</sup>F-labeled setoperone. *J Neurochem* 1990;54:1744-1754.
- Biver F, Goldman S, Luxen A, et al. Multicompartmental study of fluorine-18 altanserine binding to brain 5HT<sub>2</sub> receptors in humans using positron emission tomography. *Eur J Nucl Med* 1994;21:937-946.
- Lyon RA, Titeler M, Frost JJ, et al. <sup>3</sup>H-3-N-methylspiperone labels D<sub>2</sub> dopamine receptors in basal ganglia and S<sub>2</sub> serotonin receptors in cerebral cortex. *J Neurosci* 1986;6:2941-2949.
- Baldessarini RJ, Kula NS, Campbell A, Bakthavachalam V, Yuan J, Neumeyer JL. Prolonged D<sub>2</sub> antidopaminergic activity of alkylating and nonalkylating derivatives of spiperone in rat brain. *Mol Pharmacol* 1992;42:856-863.
- Sorensen SM, Kehne JH, Fadaye GM, et al. Characterization of the 5-HT<sub>2</sub> receptor antagonist MDL 100907 as a putative atypical antipsychotic: behavioral, electrophysiological and neurochemical studies. *J Pharmacol Exp Ther* 1993;266:684-691.
- Schmidt CJ, Fadaye GM. The selective 5-HT<sub>2A</sub> receptor antagonist, MDL 100,907, increases dopamine efflux in the prefrontal cortex of the rat. *Eur J Pharmacol* 1995;273:273-279.
- Kehne JH, Baron BM, Carr AA, et al. Preclinical characterization of the potential of the putative atypical antipsychotic MDL 100,907 as a potent 5HT<sub>2A</sub> antagonist with a favorable CNS safety profile. *J Pharmacol Exp Ther* 1996;277:968-981.
- Lundkvist C, Halldin C, Ginovart N, et al. [<sup>11</sup>C]MDL 100,907, a radioligand for selective imaging of 5-HT<sub>2A</sub> receptors with positron emission tomography. *Life Sci* 1996;58:PL187-PL192.
- Wienhard K, Dahlbom M, Eriksson L, et al. The ECAT EXACT HR: performance of a new high resolution positron scanner. *J Comput Assist Tomogr* 1994;18:110-118.
- Bergström M, Boethius J, Eriksson L, Greitz T, Ribbe T, Widen L. Head fixation device for reproducible position alignment in transmission CT and positron emission tomography. *J Comput Assist Tomogr* 1981;5:136-141.
- Eriksson L, Holte S, Bohm C, Kesselberg M, Hovander B. Automatic blood sampling systems for positron emission tomography. *IEEE Trans Nucl Sci* 1988;35:703-707.
- Farde L, Eriksson L, Blomquist G, Halldin C. Kinetic analysis of central [<sup>11</sup>C]raclopride binding to D<sub>2</sub>-dopamine receptors studied by PET: a comparison to the equilibrium analysis. *J Cereb Blood Flow Metab* 1989;9:696-708.
- Swahn C-G, Halldin C, Farde L, Sedvall G. Metabolism of the PET ligand [<sup>11</sup>C]SCH23390. Identification of two radiolabelled metabolites with HPLC. *Hum Psychopharmacol* 1994;9:25-31.
- Halldin C, Swahn C-G, Farde L, Sedvall G. Radioligand disposition and metabolism: key information in early drug development. In: Comer D, ed. *PET for drug development and evaluation*. Dordrecht, The Netherlands: Kluwer Academic Publisher; 1995:55-65.
- Mintun MA, Raichle ME, Kilbourn MR, Wooten GF, Welch MJ. A quantitative model for the in vivo assessment of drug binding sites with positron emission tomography. *Ann Neurol* 1984;15:217-227.
- Huang SC, Barrio JR, Phelps ME. Neuroreceptor assay with positron emission tomography: equilibrium versus dynamic approaches. *J Cereb Blood Flow Metab* 1986;6:515-521.
- Wong DF, Gjedde A, Wagner HN Jr. Quantification of neuroreceptors in the living human brain. I. Irreversible binding of ligands. *J Cereb Blood Flow Metab* 1986;6:137-146.
- Laruelle M, Baldwin RM, Rattner Z, et al. SPECT quantification of [<sup>123</sup>I]iomazenil binding to benzodiazepine receptors in nonhuman primates: I. Kinetic modeling of single bolus experiments. *J Cereb Blood Flow Metab* 1994;14:439-452.
- Marquardt D. An algorithm for least-squares estimation of nonlinear parameters. *J Soc Ind Appl Math* 1963;11:431-441.
- Onishi Y, Yonekura Y, Mukai T, et al. Simple quantification of benzodiazepine receptor binding and ligand transport using iodine-123-iomazenil and two SPECT scans. *J Nucl Med* 1995;36:1201-1210.
- Schotte A, Maloteaux JM, Laduron PM. Characterization and regional distribution of serotonin S<sub>2</sub>-receptors in human brain. *Brain Res* 1983;276:231-235.
- Hoyer D, Pazos A, Probst A, Palacios JM. Serotonin receptors in the human brain. II. Characterization and autoradiographic localization of 5-HT<sub>1C</sub> and 5-HT<sub>2</sub> recognition sites. *Brain Res* 1986;376:97-107.
- Pazos A, Probst A, Palacios JM. Serotonin receptors in the human brain-IV. Autoradiographic mapping of serotonin-2 receptors. *Neuroscience* 1987;21:123-139.
- Akaike H. A new look at the statistical model identification. *IEEE Trans Automat Contr* 1974;19:716-723.
- Schwarz G. Estimating the dimension of a model. *Ann Stat* 1978;6:461-464.
- Hawkins RA, Phelps ME, Huang SC. Effects of temporal sampling, glucose metabolic rates, and disruptions of the blood-brain barrier on the FDG model with and without a vascular compartment: studies in human brain tumors with PET. *J Cereb Blood Flow Metab* 1986;6:170-183.
- Koeppel RA, Mangner T, Betz AL, et al. Use of [<sup>11</sup>C]aminocyclohexanecarboxylate for the measurement of amino acid uptake and distribution volume in human brain. *J Cereb Blood Flow Metab* 1990;10:727-739.
- Leenders KL, Perani D, Lammertsma AA, et al. Cerebral blood flow, blood volume and oxygen utilization. Normal values and effect of age. *Brain* 1990;113:27-47.
- Logan J, Fowler JS, Volkow ND, et al. Graphical analysis of reversible radioligand binding from time-activity measurements applied to [<sup>11</sup>C-methyl]-(-)-cocaine PET studies in human subjects. *J Cereb Blood Flow Metab* 1990;10:740-747.
- De Clerck F, Xhonneux B, Leysen J, Janssen PA. Evidence for functional 5-HT<sub>2</sub> receptor sites on human blood platelets. *Biochem Pharmacol* 1984;33:2807-2811.
- Blin J, Baron JC, Dubois B, et al. Loss of brain 5-HT<sub>2</sub> receptors in Alzheimer's disease. In vivo assessment with positron emission tomography and [<sup>18</sup>F]setoperone. *Brain* 1993;116:497-510.